Hindawi
Advances in Materials Science and Engineering
Volume 2023, Article ID 9867691, 1 page
https://doi.org/10.1155/2023/9867691

Retraction

Retracted: Multilayered Electroactive Polyaniline-ZnO Modified GCE for Electrochemical Detection of Paracetamol

Advances in Materials Science and Engineering

Received 26 December 2023; Accepted 26 December 2023; Published 29 December 2023

This article has been retracted by Hindawi, as publisher, following an investigation undertaken by the publisher [1]. This investigation has uncovered evidence of systematic manipulation of the publication and peer-review process. We cannot, therefore, vouch for the reliability or integrity of this article.

Please note that this notice is intended solely to alert readers that the peer-review process of this article has been compromised.

Wiley and Hindawi regret that the usual quality checks did not identify these issues before publication and have since put additional measures in place to safeguard research integrity.

We wish to credit our Research Integrity and Research Publishing teams and anonymous and named external researchers and research integrity experts for contributing to this investigation.

The corresponding author, as the representative of all authors, has been given the opportunity to register their agreement or disagreement to this retraction. We have kept a record of any response received.

References

[1] S. Chufamo, B. Kelita, S. Berhanu, A. Kemal, and A. Lelago, "Multilayered Electroactive Polyaniline-ZnO Modified GCE for Electrochemical Detection of Paracetamol," *Advances in Materials Science and Engineering*, vol. 2022, Article ID 5186638, 11 pages, 2022.

Hindawi
Advances in Materials Science and Engineering
Volume 2022, Article ID 5186638, 11 pages
https://doi.org/10.1155/2022/5186638

Research Article

Multilayered Electroactive Polyaniline-ZnO Modified GCE for Electrochemical Detection of Paracetamol

Samuel Chufamo,[1] **Bezabih Kelita**,[1] **Sintayehu Berhanu**,[2] **Almaz Kemal**,[1] **and Alemu Lelago**[1]

[1]*Department of Chemistry, College of Natural and Computational Sciences, Wolaita Sodo University, P.O. Box 138, Wolaita Sodo, Ethiopia*
[2]*Department of Chemistry, College of Natural and Computational Sciences, Bonga University, P.O. Box 334, Bonga, Ethiopia*

Correspondence should be addressed to Samuel Chufamo; samuel.chuf@gmail.com and Sintayehu Berhanu; sintayehuberhanu38@gmail.com

Received 6 June 2022; Revised 12 August 2022; Accepted 29 August 2022; Published 27 September 2022

Academic Editor: Haichang Zhang

Paracetamol (PC) is widely used for defensive and medicinal purposes for human beings. But their deposition in the human body will persuade thoughtful health risks. So, the enhancement of sensitive and selective techniques for the easy and fast detection of PC is extremely fundamental. Multilayered electroactive polyaniline-ZnO nanocomposite (NC) film was developed for PC detection which was based on the oxidation of PC with polyaniline doped zinc oxide on a glassy carbon electrode (PANI/ZnO/GCE). PANI and PANI/ZnO NCs were fabricated by both electrochemical and in-situ oxidative chemical polymerization methods. The morphology of PANI/ZnO shows that the polymer was distributed on the surface of ZnO, and the XRD pattern confirms that the average size calculated was 7.48 nm for PANI/ZnO. From UV-Vis measurements, the PANI/ZnO composite shows a redshift relative to PANI and ZnO. Moreover, FT-IR spectra show that chemical bonds and stretching are assigned to different peaks. Using differential pulse voltammetry, the fabricated PANI/ZnO/GCE electrochemical sensor displays good analytical performance for PC with detection limits of 4×10^{-8} M and a sensitivity of 2.571 mA/1×10^{-8} M with a linear concentration of PC within the range of 1.0 to 7.0×10^{-8} M.

1. Introduction

Paracetamol (PC), (N-(4-hydroxyphenyl) acetamide) is a synthetic well-known compound that belongs to the class of drugs called analgesics and antipyretics [1]. It is commonly used for the cure of fever and to assuage moderate pain and migraine. But recent investigations indicate that at an optimum dose, PC does not have any side effects. However, an overdose can cause hepatotoxicity and acute kidney disease despite its apparent innocuous character [2, 3].

Therefore, the development of useful analytical tools to detect and determine PC is required. So far, different analytical methods have been utilized for the detection of PC; chemiluminescence [4], high-performance liquid chromatography [5], mass spectrometry [6], spectrophotometry [7], and electrochemical sensors have been used [8]. Most of the techniques are difficult, time-consuming processes, and they generally demand professional apparatus, except for electrochemical sensors [5, 9, 10].

Electrochemical sensors based on conducting polymer-metal oxide composite materials have piqued researchers' curiosity in recent years [11, 12]. Conducting polymers such as polyaniline (PANI), polythiophene, polypyrrole, and their derivatives are used for different applications. This is due to their chemical stability, conductivity, lightweight nature, and mechanical flexibility [12]. Among the conducting polymers, polyaniline is broadly used for its excellent properties, such as excellent conductance, easy preparation, low fabrication cost, environmental friendliness and stability, and its electrochemical redox characteristics [12–14].

PANI has three different fundamental oxidation forms: leucoemeraldine, emeraldine base, and pernigraniline. The only electrically conducting form is the emeraldine salt form, which is the protonated form of base [15–17]. Electrochemical sensors developed based on conducting PANI are used in the enhancement of community health and in monitoring the environment due to their better response characteristics, fast detection, selectivity, and sensitivity to slight changes [18]. However, it has a poor lifetime owing to the broken backbone chain. To overcome these drawbacks, inorganic nanomaterials are used in the matrix which advances their electrical conductivity, characteristics, and strength of the polymer matrix [19].

Recently, several groups reported electrochemical determination of PC based on its oxidation behavior with different electrodes such as ZrO_2NPs-modified carbon paste electrode (ZMCPE) [20], Cd(OH)2-rGO-modified glassy carbon electrode [21], nickel hexacyanoferrate-modified carbon paste electrode [22], and multiwall nanoparticle-modified glass carbon electrode (MWNT/GCE) [23]. The excellent isoelectric point, a transparent n-type semiconductor with a direct broad bandgap (3.37 eV), biocompatibility, nontoxicity, strong chemical stability, and high electron transfer capability are some of the unique qualities of nanostructured zinc oxide (ZnO) [24, 25]. The combination of ZnO nanoparticles (NPs) with the polymer matrix enhances the mechanical strength, increases the detecting ability, tunes optoelectrical properties, and changes the surface as well as the conductivity of the composite [26–29].

To the best of our knowledge, there is no study in the literature that uses PANI/ZnO nanocomposites (NCs) as an electrochemical sensor for PC detection. Thus, this research was deliberated to fabricate PANI, ZnO NPs, and PANI/ZnO NCs on GCE via layer-by-layer electrochemical polymerization of aniline. Then, the fabricated NCs were characterized by using an X-ray diffractometer (XRD), an FT-IR spectrophotometer, a UV-Vis spectrophotometer, and a scanning electron microscope (SEM). The sensitivity and selectivity of the NCs to PC detection were studied by using cyclic voltammetry and differential pulse voltammograms.

2. Experimental

2.1. Materials. $Zn(NO_3)_2{\cdot}6H_2O$ (99.0% purity), NaOH (≥98% purity), aniline, ammonium peroxodisulfate (APS) sodium dihydrogen phosphate (98%), disodium hydrogen phosphate (98%), hydrochloric acid (35–37%), potassium nitrate (99%), paracetamol, argon gas (99.9%) were purchased from India and doubly distilled water were used during the experiment.

2.2. Synthesis of ZnO Nanoparticles. ZnO NPs were synthesized by using the [30] reported method. 2.9749 g of $Zn(NO_3)_2{\bullet}6H_2O$ was first dissolved in 200 ml of distilled water to make a precursor solution containing 0.05 M Zn-solution. On a heated plate at 80°C, the solution was magnetically swirled for 15 minutes. 2.0 M NaOH solutions were made in a separate beaker by dissolving 12 g of NaOH pellets in 250 ml of distilled water. The solution was then magnetically stirred at room temperature for 10 minutes.

After that, 40 mL of NaOH solution was added to the Zn solution while stirring. The formation of a white precipitate began almost immediately. The white precipitate bleached the entire solution. At 80°C, the mixture was constantly stirred for another 30 minutes before being allowed to cool to room temperature. Then, the precipitate was collected by filtering, rinsed several times with distilled water, dried overnight in the open air, and calcined in air at 200°C and then at 500°C for 2 h.

2.3. Chemical Synthesis of PANI and PANI/ZnO Composite. Polyaniline was chemically synthesized following the procedure reported by Alam et al. [31]. 20 mL distilled aniline was added to 250 mL 1 M HCl in a round bottom flask at 27°C for 30 min while stirring, and then 125 mL 1 M APS solution was added dropwise. Following the addition of APS, the reaction mixture was stirred constantly for 4 hours at 0–4°C, resulting in a thick green solution that was stored for 24 hrs. To remove oligomers, the precipitate was washed with 1 M HCl. PANI was then dried for 24 hours in a vacuum oven at 60°C (emeraldine).

In-situ oxidation polymerization was used to make PANI/ZnO NCs following the procedure reported by Yerawar et al. [32]. 2 g of ZnO was added to 20 mL of aniline produced in 1 M aqueous hydrochloric acid and agitated for half an hour before allowing settling for another half hour. Ammonium persulphate (APS) was added to this solution as an oxidant produced in aqueous hydrochloric acid (1 M) dropwise for half an hour at 4°C with continual stirring.

The ratio of the monomer to the oxidizing agent was kept constant at 1:1.25. After eight hours of stirring, the dark green slurry was maintained overnight and then filtered. To remove the excess initiator, monomer, and oligomer, the precipitated polymer was washed with distilled water until the filtrate was colorless, then with acetone and methanol. Finally, the polymer was dried in the air for roughly a day before being baked for 15 hrs at 80°C.

Electrochemical characterization of chemically synthesized PANI and PANI/ZnO NCs was carried out using cyclic voltammetry. The GCE was polished with 0.05 M alumina powder, cleaned with distilled water, ultrasonicated with deionized water and ethanol, and dried at room temperature before being drop-coated with synthetic nanomaterials. 2 mg of PANI was dissolved in 2 mL of ethanol and ultrasonically stirred. The aforementioned suspension was then drop-coated onto the surface of a bare glassy carbon electrode and allowed to dry at ambient temperature.

Then, the measurements were performed in 1 M HCl in the potential range from −0.5 V to +1.1 V, and scan rates were 30, 40, 50, 60, 70, and 80 mVs^{-1}. Similarly, 2 mg of PANI/ZnO was dissolved in 2 mL of ethanol followed by sonication and was drop-coated on the bare electrode to obtain PANI/ZnO/GCE. The characterization was a similar condition as PANI/GCE.

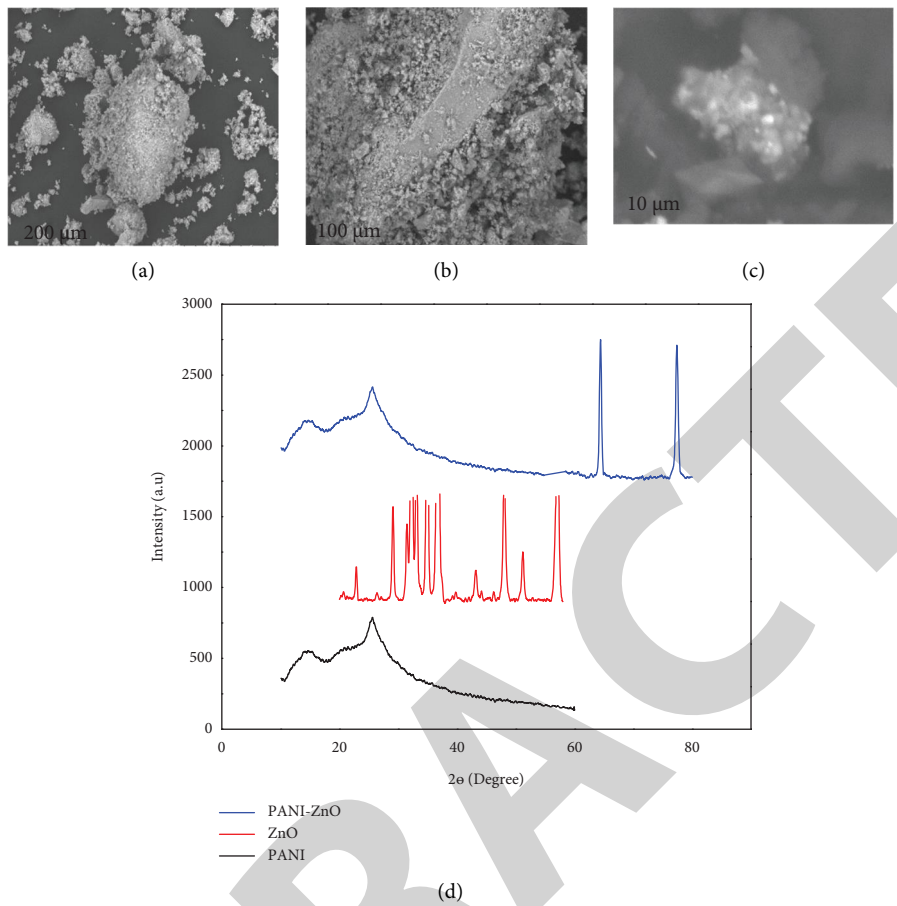

Figure 1: SEM micrographs of (a) ZnO, (b) PANI, (c) PANI/ZnO, (d) XRD spectra of ZnO, PANI, and PANI/ZnO NCs.

2.4. Electrochemical Synthesis of Multilayered Electroactive PANI-ZnO/GCE. In a single compartment cell, potentiodynamic electrochemical polymerization of aniline (0.1 M) in 1 M HCl aqueous solution was performed with a glassy carbon electrode (GCE) as the working electrode, a platinum wire counter electrode, and Ag/AgCl as the reference electrode. Before polymerization, the glassy carbon electrode (GCE) working electrode was polished with 0.05 μm alumina powder to get a shiny surface and rinsed with distilled water followed by ultrasonication with ethanol and deionized water, respectively, and then dried at room temperature.

Before electrochemical polymerization, the solution containing the monomer was purged with argon and an overflow of argon was maintained during electropolymerization. Electropolymerization was performed by 10 potential cycles carried out within the potential range −0.5 to 1.2 V. Thus, the formed PANI polymer on the GCE surface was washed with deionized water before characterization by CV. After 10 cycles of electropolymerization of PANI in 1 M, HCl containing 0.1 M of aniline monomers, 5 μL of ZnO suspension was drop-coated on the PANI/GCE surface and dried for 30 min. Then, the electrode was transferred back into the aniline solution, and additional electrochemical polymerization was carried out by 5 potentiodynamic cycles with the same scan rate of 50 mVs^{-1} and within the same potential range of −0.5 to 1.2 V.

2.5. Structural and Electrochemical Characterization. FT-IR and scanning electron microscopy (SEM) were used to examine the functional groups and morphology of the NCs. The FT-IR spectrum was measured on Spectrum65 FT-IR (PerkinElmer) in the range from 4000 to 400 cm^{-1}. The morphologies of the NCs were measured by EVO 18 SEM. The absorbance measurements were conducted by using the SPECTRONIC GENESYS 2PC UV-Vis spectrophotometer. All electrochemical measurements were conducted by Bass 100 three-electrode systems.

2.6. Optimization of PAN-ZnO/GCE as an Electrochemical Sensor. In the presence of a supporting electrolyte (0.1 M phosphate buffer solution and 0.1 mol/L KCl), the influence of pH on the oxidation peak current of PC was investigated in the pH range of 4.0 to 8.0. The concentration of PC was optimized with different concentration ranges (1, 5, 10, 20, 30, 40, 50, 60, 80, and 100 μM).

3. Results and Discussion

3.1. Structural Characterization

3.1.1. XRD Pattern. The structure and crystallite size of the fabricated materials were characterized by XRD. Figure 1(d) demonstrates the XRD patterns of pure PANI,

ZnO, and the PANI-ZnO composite. The XRD pattern of PANI shows a broad peak at $2\theta = 20.4^{\circ}$ and 24.14° which is related to the (200) and (110) planes of PANI [33, 34]. The XRD patterns of ZnO and PANI–ZnO NCs illustrates the typical peaks for crystalline ZnO of wurtzite structured with a hexagonal shape which is reliable with the JCPDS file of ZnO. This shows that the existence of PANI did not change the crystalline structure of ZnO. All the diffraction peaks of PANI/ZnO NCs moderately shift to larger values of 2θ and show the amorphous nature obviously with good reflections related to ZnO. The average size calculated was 7.48 nm, and the small size is due to the intermolecular interaction between conducting ZnO NPs and PANI [34–40].

3.1.2. Scanning Electron Microscope. The morphology of PANI, ZnO NPs, and PANI/ZnO NCs were displayed in Figure 1. Figure 1(a) shows the surface morphology of the ZnO NPs; it displays that the particles are fine with bright spots. Figure 1(b) illustrates the polyaniline surface morphology, which shows particle separation as well as it is not heavily influenced by agglomeration. The interaction of ZnO NPs with the polyaniline matrix is seen in Figure 1(c). The morphology of PANI has changed with the additions of ZnO NPs, and the particles are separated smoothly and are not highly affected by agglomeration.

3.1.3. FT-IR Spectra. The FT-IR spectra of PANI and PANI/ZnO is shown in Figure 2(d). In PANI/ZnO spectra, the peak at 1576 cm^{-1} and 1475 cm^{-1} indicates the presence of quinoid and benzenoid rings, respectively. The C-C ring's asymmetric and symmetric stretching vibrations are ascribed to the peaks at 1475 cm^{-1} and 1294 cm^{-1}, and the peak at 2921 cm^{-1} represents the C-H stretching mode of vibration.

In the FT-IR spectrum of the PANI/ZnO NCs, there is shifting of some absorption peaks to a higher wavenumber relative to the spectrum of PANI, and the peak change from 3458 to 3430 cm^{-1}, 2928 to 2921 cm^{-1}, 1475 to 1473 cm^{-1}, and 1121 to 1107 cm^{-1} is due to the presence of ZnO NPs in the aniline polymer matrix. The interaction between ZnO and PANI is attributed to the creation of hydrogen bonds between H-N at 3430 cm^{-1} and the oxygen of ZnO, resulting in a peak at 802 cm^{-1} [33, 36, 38].

3.1.4. UV-Vis Spectra. The UV-Vis spectra of ZnO, PANI, and PANI/ZnO NCs were obtained by using diffuse reflectance spectroscopy (DRS) with $BaSO_4$ as a reference. The bandgap (Eg) can be estimated by Kubelka–Munk functions versus photon energy given by

$$(F(r)(h\nu))^2 = \left(\frac{(1-R)^2}{2R}(h\nu)\right)^2 vs\, h\nu, \quad (1)$$

where $h\nu$ is photon of energy with ν-frequency and h-Plank's constant, and R is reflectance data from the DRS data.

The optical band gap graphs for ZnO, PANI, and PANI/ZnO are given in Figures 2(a)–2(c). The calculated bandgap energy of ZnO, PANI, and PANI/ZnO was 3.19, 2.50, and 2.36 eV, respectively. The bandgap energy (2.50 eV) in the case of PANI is the same as in some previous literature [41, 42]. Additions of ZnO into PANI allow the bandgap of PANI to decrease, and this is due to the interaction between PANI and ZnO, which caused alterations in the polyaniline chain's electron density. This suggests an improvement in the electrical and optical properties of NCs [39, 43].

3.2. Electrochemical Characterization

3.2.1. Electrodeposition of PANI-ZnO Composite on the Glassy Carbon Electrode. Figure 3(a) shows cyclic voltammograms measurements on GCE during electropolymerization of aniline in 0.1 M HCl aqueous solution for 10 cycles at a scan rate of 50 mVs^{-1} in the potential range of −0.5 V to 1.2 V. During the forward scan, the first cycle was characterized by the irreversible oxidation of aniline. When the potential was switched in the reverse scan, three cathodic waves appeared. As read from the last polymerization cycle, there are three redox peaks (A/A', B/B', and C/C'); the three anodic peaks occurred at 0.356, 0.538, and 0.783 V, and three cathodic peaks occurred at 0.076, 0.456, and 0.631 V vs. Ag/AgCl for the first, second, and third waves, respectively. Aniline was polymerized on PANI/ZnO/GCE for 5 cycles at the same voltage and scan rate after a drop coating of 5 μL ZnO suspensions on PANI/GCE and drying for 30 minutes.

Figure 3(b) shows three redox peaks and radical formation in first cycle polymerization; this shows that aniline monomers are fully polymerized. The three redox peaks of aniline show different fundamental oxidation forms: leucoemeraldine (fully reduced), emeraldine base (half oxidized) which is electrically conductive, and pernigraniline (fully oxidized). The fabricated PANI/ZnO/GCE electrode was characterized in 0.1 M HCl solution at a potential range of −0.5 to 1.1 V and 50 mVs^{-1} scan rate. Figure 3(c) shows a peak of current increases as scan rate increases; this indicates that PANI/ZnO NCs has good catalytic activities between GCE and HCl electrolyte.

The plot between oxidation peak potential (Epa) and scan rate (ln ν) is also shown in Figure 3(d). It can be seen that plotting of the Epa *vs.* ln ν of PANI/ZnO/GCE gives a straight line with equation $\mathrm{Epa} = 0.05077\ln\nu + 0.255$ and linear regression $R = 0.995$ by using redox peak. The electrode reaction was a surface controlled reaction process, and the anodic peak potential shifted positively as the scan rate increased.

3.2.2. Electrochemical Properties of Chemically Synthesized PANI/GCE and PANI/ZnO/GCE. The synthesized PANI and PANI/ZnO NCs were sonicated; 5 μL was drop-coated on the GCE to produce PANI/GCE and PANI/ZnO/GCE, respectively. The synthesized electrodes were characterized in 1 M HCl by applying cyclic voltammetry (CV) within the potential range of −500 to 1100 mV, and the scan rate changed from 40 to 100 mVs^{-1}. Figures 4(a) and 4(b) showed two anodic and two cathodic peaks for electrochemically formed films (A/A' and B/B'). Linear relationship was observed between the scan rate and the peak current of the material.

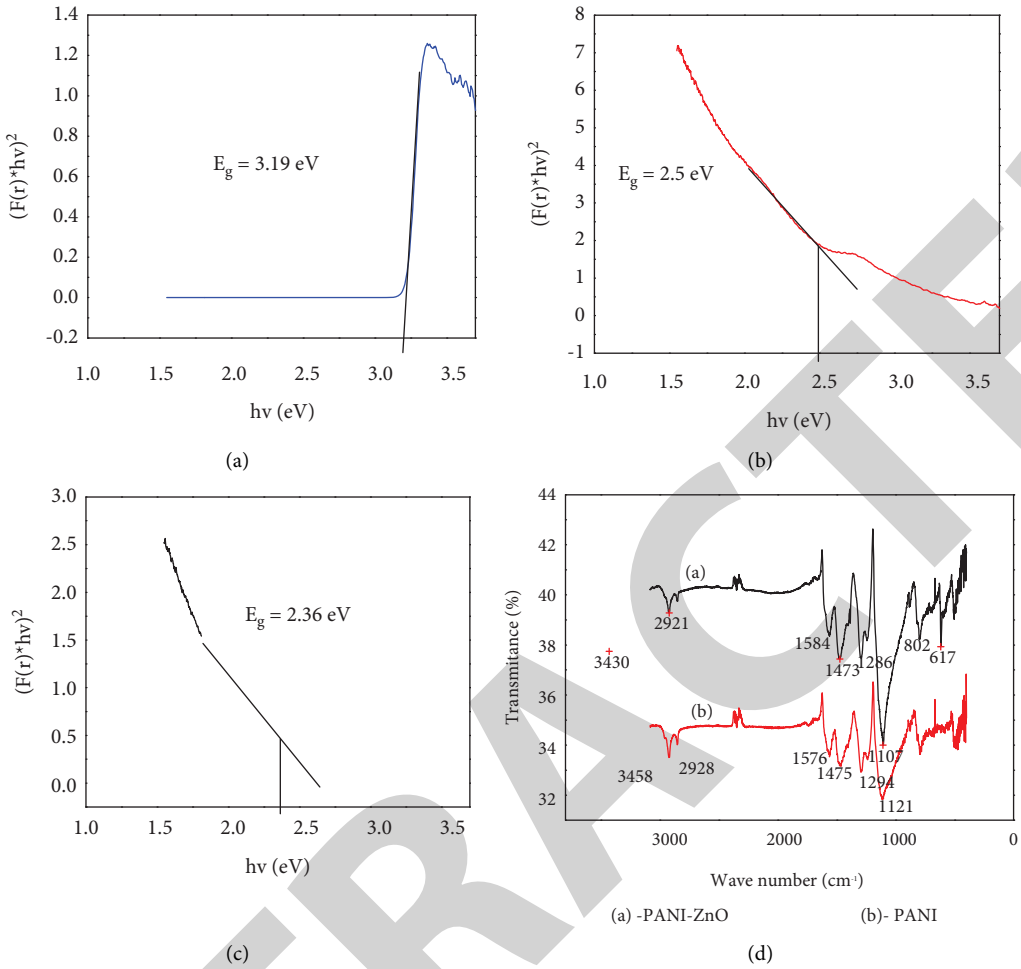

Figure 2: Kubelka–Munk functions versus photon energy for (a) ZnO, (b) PANI, (c) PANI-ZnO composite, and (d) FT-IR spectra of PANI/ZnO.

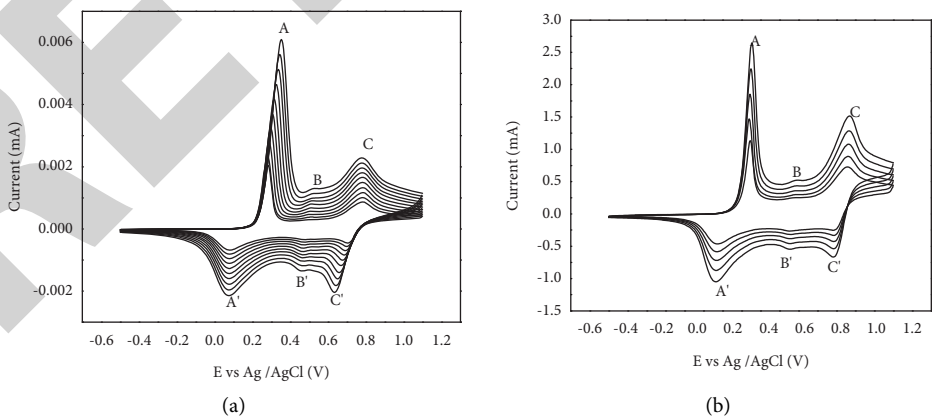

Figure 3: Continued.

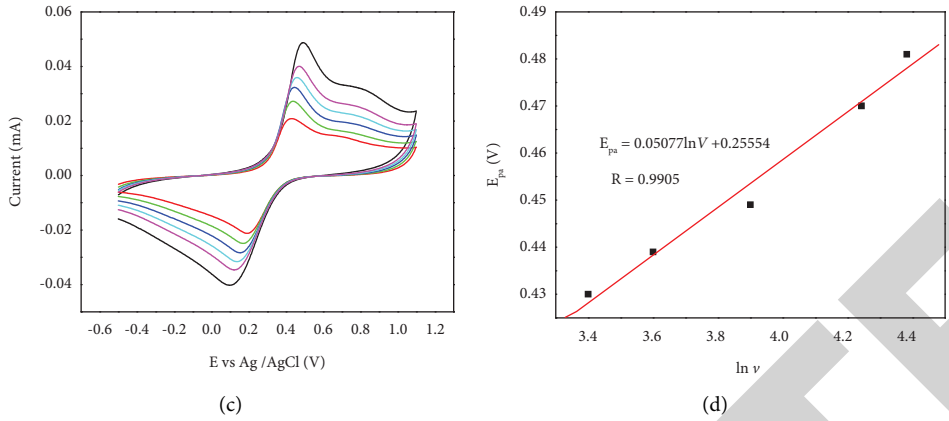

FIGURE 3: Electrochemical polymerization of 0.1 M aniline in 1 M HCl, at a scan rate of 50 mVs^{-1} in the potential range of −0.5 V to 1.1 V for 10 cycles for (a) GCE and 5 cycles for (b) PANI ZnO/GCE, (c) CV in 0.1 M HCl from −0.5 V to 1.1 V, and (d) Epa vs. lnv at different scan rates of 30, 40, 50, 60, 70, and 80 mVs^{-1} of PANI-ZnO/GCE.

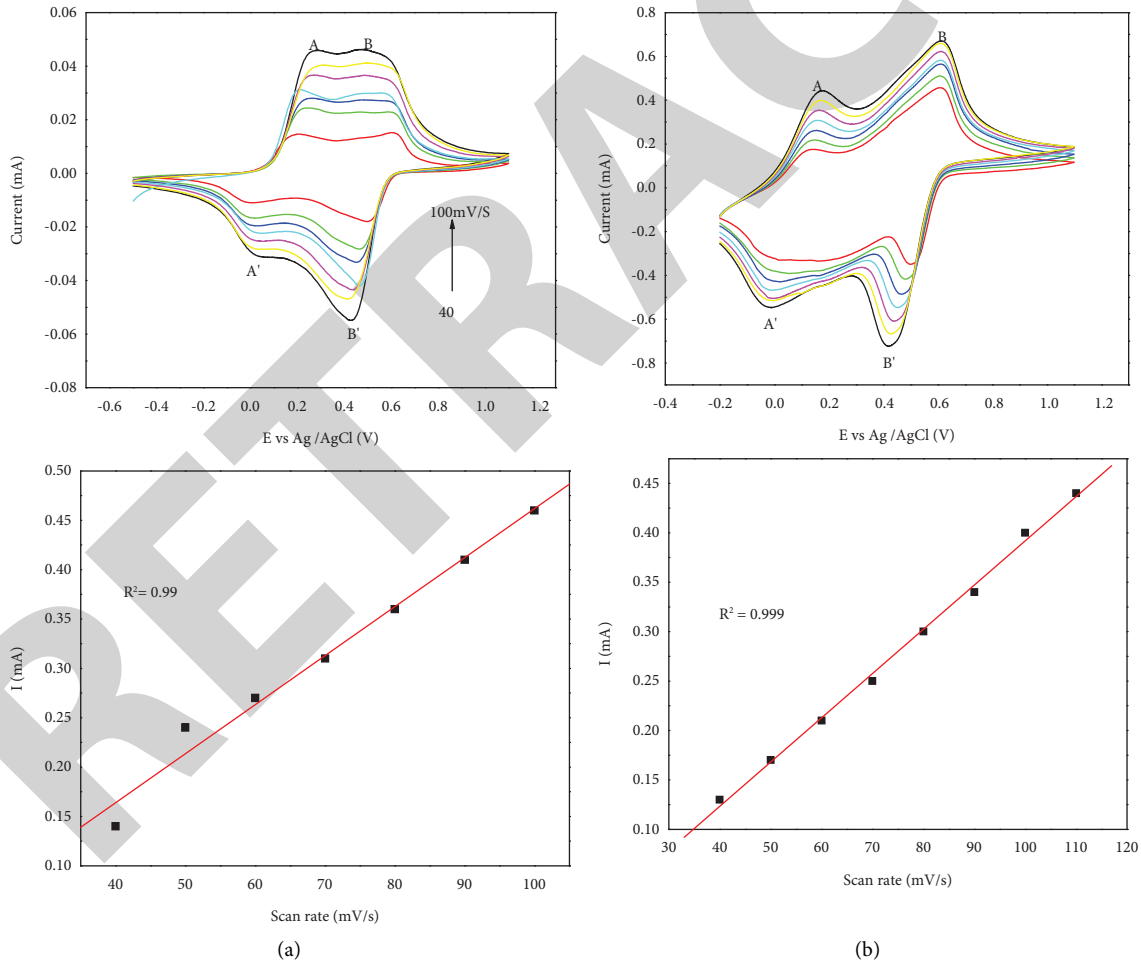

FIGURE 4: Cyclic voltammogram characterization of chemically synthesized (a) PANI and (b) PANI-ZnO in 1 M HCl at different scan rates (40, 50, 60, 70, 80, 90, and 100 mVs^{-1}) and a plot of the scan rate dependence of their anodic peak (first peaks) currents (a' and b').

The response of PANI/GCE and PANI/ZnO/GCE electrodes showed a change in the scan rate, and the peak current increased as the scan rate increased. The plot of the anodic peak currents as a function of the potential scan rate for the first peak of Figures 4(a) and 4(b) is shown in Figures 4(a) and 4(b). The linear correlation suggested that the NCs were electroactive, conducting, and restricted to the electrode's surface. The fabricated PANI/ZnO/GCE

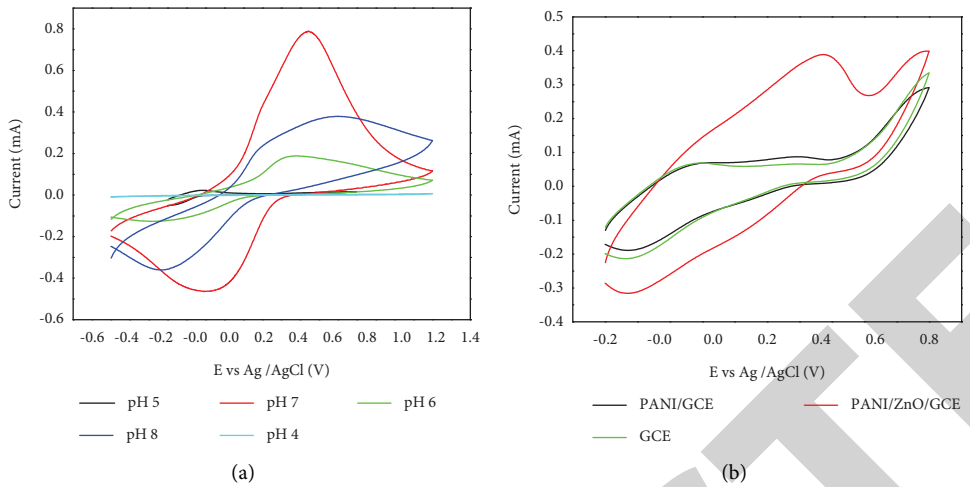

FIGURE 5: (a) CV of 40 μM PC at PANI/ZnO/GCE in 0.1 M PBS with different pH values of 4.0, 5.0, 6.0, 7.0, and 8.0 at a scan rate of 50 mVs^{-1} and (b) typical CV of 40 μM of PC in 0.1 M PBS, pH 7.0 at PANI-ZnO/GCE, PANI/GCE, and GCE.

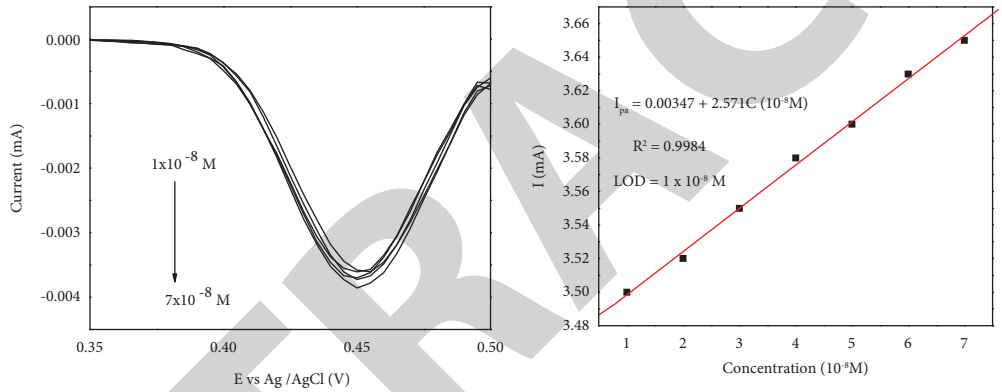

FIGURE 6: (a) Differential pulse voltammogram of PC at different concentrations range (1, 2, 3, 4, 5, 6, and 7×10^{-8} M) at PANI/ZnO/GCE in 0.1 M PBS (pH 7.0). (b) Calibration plot of oxidation peak current vs. PC concentration.

electrode in Figure 4(b) shows a small peak-to-peak separation than the PANI/GCE electrode in Figure 4(a). The small peak-to-peak separation of PANI/ZnO reveals that an NC film was more electroactive, facilitating the electron transfer process and excellent conductibility than PANI NCs.

3.2.3. Cyclic Voltammetric Study of Paracetamol on PANI-ZnO/GCE

Effect of pH. The stability of the sensor is central; the effect of pH on the redox reaction of PC at the fabricated electrode was studied in the pH range from 4 to 8. The relationship between chemical oxidation efficiency and pH of the solution was obtained by CV; the results are shown in Figure 5(a). From the graph, the oxidation peak current of PC increased with increasing pH up to 7. But after reaching the maximum, the oxidation peak decreases as pH of solution changes from 7. Therefore, the fabricated electrode is inactive and cannot sense the drug. But at neutral pH, there is no protonation or deprotonation of PANI/ZnO/GCE and PC. Consequently, we chose neutral pH as the experimental condition.

3.2.4. Cyclic Voltammetry of Paracetamol at Different Electrodes.

Using cyclic voltammetry, the electrochemical behavior of 40 M PC at the bare GCE, PANI/GCE, and PANI/ZnO/GCE was explored for comparison in phosphate buffer at a pH of 7.0, and the findings are given in Figure 5(b).

The oxidation peak of PC can be seen with a potential range of −0.2 V to 0.8 V at the GCE, PANI/GCE, and PANI/ZnO/GCE. Comparing PANI/GCE and GCE with PANI/ZnO/GCE, it had a higher anodic peak current and voltammetric response. This could be owing to the huge surface area and strong conductivity of the PANI/ZnO-modified electrode, as well as the good integration of ZnO NPs and PANI films or synergetic effect and combinational electrochemical catalytic properties of the synthesized PANI and ZnO NPs.

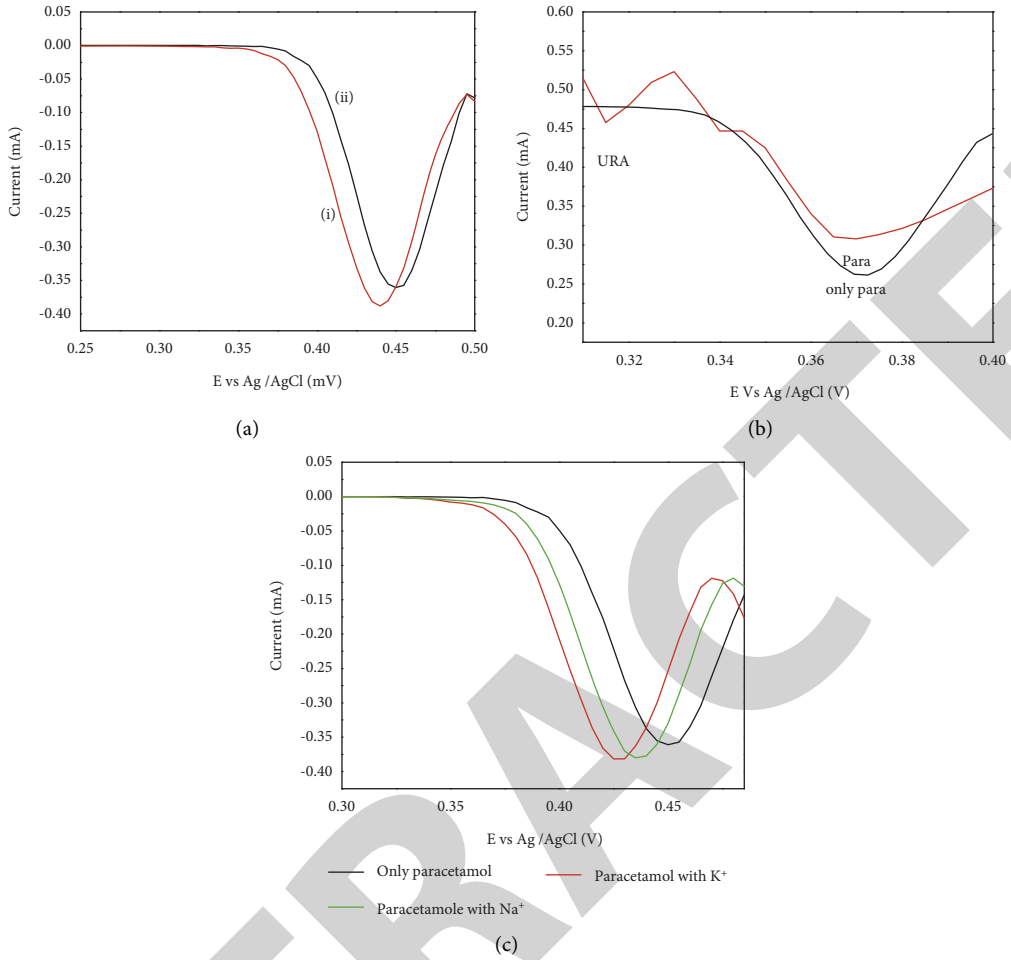

Figure 7: (a) The stability of the PANI-ZnO/GCE by differential pulse voltammogram peak "*a*" first-day modification of the electrode and peak "*b*" after ten weeks using the same electrode. Interference study of 0.1 M of PBS (pH = 7.0) containing 1.0×10^{-8} M PC and using PANI-ZnO/GCE at a scan rate of 50 mV/s for 1.0×10^{-8} M (b) of uric acid, and (c) Na^+ and K^+ ion.

3.3. Electrochemical Determination of Paracetamol Using DPV. The voltammetric determination of PC was conducted with a three-electrode setup in 0.1 M PBS (pH 7.0) and with PANI/ZnO/GCE as a working electrode. The effect of varying PC concentrations (1.0, 2.0, 3.0, 4.0, 5.0, 6.0, 7.0 × 10–8 M) at PANI/ZnO/GCE was studied by using differential pulse voltammograms (DPVs) and illustrated in Figure 6(a) under the optimum experimental conditions of pH 7.0. The resulting differential voltammogram current peaks and the height of these current peaks are directly proportional to the PC concentration within the range of 1–7 x 10–8 M, and the linear regression equation is found Ipa/mA = 2.571 C (1 × 10–8 M) + 0.00347 ($R2 = 0.9984$).

The sensitivity of the PANI/ZnO/GCE was calculated from the slope of the curve, and it has been found 2.571 mA/1.0×10^{-8} M. The magnitude of the determination limit of the PANI/ZnO/GCE fabricated electrochemical sensor for PC was calculated by using the formula; LOD = $3\delta/m$, where δ represents the standard deviation and m is the slope of the calibration curve. The determination limit was found to be 1×10^{-8} M, and the limit of quantification (LOQ) was calculated by using the equation: LOQ = 10 (δ/m). The limit of quantification value was found to be 0.3×10^{-7} M.

Table 1: Determination of PC from waste water effluent using the PANI-ZnO/GCE chemical sensor.

Amount of PC (M)	Found (M)	Recovery (%)
1×10^{-8}	9.7×10^{-9}	97
2×10^{-8}	1.95×10^{-8}	97.5
3×10^{-8}	3.2×10^{-8}	106

3.4. Reproducibility, Stability, and Interference Study. The reproducibility of fabricated PANI/ZnO NC on the GCE PC electrochemical sensor is shown in Figure 7(a). The long-term stability of the fabricated electrode was studied after storage in the air for ten weeks at room temperature, and the result shows that about 10% of its initial current was lost. This shows that the PANI/ZnO film did not peel off easily from the surface of the GCE, and electroactive PANI was strongly coated on the GCE. The electrochemical sensor developed for the detection of PC may be affected by

Table 2: Comparison of present study results of analytical parameters with recently reported for detection of PC over various modified electrodes.

Modified electrodes	Techniques	LOD	References
GCE	DPV	8.69×10^{-7}M	[44]
AGCE	DPV	8×10^{-8} M	[36]
MWNT/GCE	DPV	0.8 μM	[23]
NiHCFMCPE	CV	8.89×10^{-8} M	[22]
Nanorods-like $Cd(OH)_2$-rGO/GCE	DPV	0.08 μM	[21]
ZrO_2NPs/MCPE (ZMCPE)	DPV	0.68 μM	[20]
PANI/ZnO/GCE	DpV	4×10^{-8} M	The present study

interference; metallic cations such as K^+, Cu^{+2}, and Na^+ and organic compounds such as p-aminophenol, caffeine, ascorbic acid, uric acid, and glucose were used for interference studies [44]. From these interferences, uric acid was used for our studies on the PANI/ZnO working electrode.

Selectivity of the electrode was examined by using PBS (pH = 7.0), containing an equal amount of 1.0×10^{-8} M of PC and 1×10^{-8} mol L^{-1} of uric acid as an interference. As shown in Figure 7(b), the voltammogram displays good peak separation from PC while the presence of uric acid affects the peak of PC by decreasing the peak current and by broadening the peak of PC. Similarly, we know that the electrochemical properties of PANI arise from oxidation and protonation of the nitrogen element of the polymer backbone, which is reactive with protons and metallic cations. From metallic ion interferences, K^+ and Na^+ were used for our studies. Selectivity of the electrode was examined by using the same procedure as for uric acid except for sodium nitrate ($NaNO_3$) and potassium nitrate (KNO_3) (1.0×10^{-8} M). As shown in Figure 7(c), the presence of Na^+ reduces the peak potential of PC by 0.026%, and the presence of K^+ reduces the peak potential by 0.051%. Therefore, the effects of metal ions (Na^+ and K^+) on the sharpness and peak potential of PC are negligible:

3.5. Analysis of the Real Sample. The fabricated PANI-ZnO/GCE electrochemical sensor was applied to detect PC in a real environmental sample. The water sample was collected from Wolaita Sodo University Teaching Referral Hospital effluent. The sample was spiked with appropriate amounts of standard PC solutions. The recovery was investigated by comparing the current response of the extracted sample against the spiked concentrations of standard PC in PBS at pH 7.0.

The results were obtained from 97% to 106%. As observed from the electrochemical analysis data in Table 1, the developed PANI-ZnO/GCE sensor is acceptable and applicable for the detection of PC. A comparison between this work and other reported literature for sensing in detection limit (LOD) is also summarized in Table 2. It shows better performance relative to other results reported in the literature.

4. Conclusion

The developed electrochemical sensor made up of ZnO film with polyaniline and deposited onto a glassy carbon electrode was successfully used for detecting PC. The cyclic voltammetry measurements show that the synthesized PANI-ZnO/GCE was more electroactive than PANI/GCE and GCE due to the high surface area and good conductive nature of PANI/ZnO. It also has a good determination limit, high stability, and good sensitivity. The DPV result shows the sensor has good analytical sensitivity (2.571 mA/1×10^{-8} M) and a limit of detection (4×10^{-8} M). Therefore, the developed electrochemical sensor produced a new approach to be used in sensors designed for the detection of PC antibiotics.

Data Availability

No data were used to support this study.

Conflicts of Interest

The authors declare that they have no conflicts of interest.

Acknowledgments

The authors would like to acknowledge the Department of Chemistry, Haramaya University for CV and DPV measurements. Also, the authors acknowledge Wolaita Sodo University Research office for financial support.

References

[1] E. Noviana, D. B. Carrão, R. Pratiwi, and C. S. Henry, "Emerging applications of paper-based analytical devices for drug analysis: a review," *Analytica Chimica Acta*, vol. 1116, pp. 70–90, 2020.

[2] E. Kozer and G. Koren, "Management of paracetamol overdose," *Drug Safety*, vol. 24, no. 7, pp. 503–512, 2001.

[3] M. T. Olaleye and B. J. Rocha, "Acetaminophen-induced liver damage in mice: effects of some medicinal plants on the oxidative defense system," *Experimental & Toxicologic Pathology*, vol. 59, no. 5, pp. 319–327, 2008.

[4] W. Ruengsitagoon, S. Liawruangrath, and A. Townshend, "Flow injection chemiluminescence determination of paracetamol," *Talanta*, vol. 69, no. 4, pp. 976–983, 2006.

[5] U. D. Pawar, A. V. Naik, A. V. Sulebhavikar, T. A. Datar, and K. Mangaonkar, "Simultaneous determination of aceclofenac, paracetamol and chlorzoxazone by HPLC in tablet dose form," *E-journal of Chemistry*, vol. 6, no. 1, pp. 289–294, 2006.

[6] T. Belal, T. Awad, and R. Clark, "Determination of paracetamol and tramadol hydrochloride in pharmaceutical mixture using HPLC and GC-MS," *Journal of Chromatographic Science*, vol. 47, no. 10, pp. 849–854, 2009.

[7] S. L. Borisagar, U. P. Jayswal, H. U. Patel, and C. N. Patel, "A validated high-performance thin layer chromatography method for estimation of lornoxicam and paracetamol in their combined tablet dosage form," *Pharmaceutical Methods*, vol. 2, no. 2, pp. 83–87, 2011.

[8] R. Rama, S. Meenakshi, K. Pandian, and S. C. B. Gopinath, "Room temperature ionic liquids-based electrochemical sensors: an overview on paracetamol detection," *Critical Reviews in Analytical Chemistry*, vol. 52, no. 6, pp. 1422–1431, 2021.

[9] X. Kang, J. Wang, H. Wu, J. Liu, I. A. Aksay, and Y. Lin, "A graphene-based electrochemical sensor for sensitive detection of paracetamol," in *Talanta*vol. 81, no. 3, pp. 754–759, 2010.

[10] M. Salajegheh, M. Kazemipour, M. M. Foroghi, and M. Ansari, "Morphine sensing by a green modified molecularly imprinted poly L-lysine/sodium alginate-activated carbon/glassy carbon electrode based on computational design," *Electroanalysis*, vol. 31, no. 3, pp. 468–476, 2019.

[11] D. Ji, Z. Liu, L. Liu et al., "Smartphone-based integrated voltammetry system for simultaneous detection of ascorbic acid, dopamine, and uric acid with graphene and gold nanoparticles modified screen-printed electrodes," *Biosensors and Bioelectronics*, vol. 119, pp. 55–62, 2018.

[12] S. Ebrahim, R. El-Raey, A. Hefnawy, H. Ibrahim, M. Soliman, and T. M. Abdel-Fattah, "Electrochemical sensor based on polyaniline nanofibers/single wall carbon nanotubes composite for detection of malathion," *Synthetic Metals*, vol. 190, pp. 13–19, 2014.

[13] M. Gerard, A. Chaubey, and B. D. Malhotra, "Application of conducting polymers to biosensors," *Biosensors and Bioelectronics*, vol. 17, no. 5, pp. 345–359, 2002.

[14] M. R. Karim, M. M. Alam, M. O. Aijaz, A. M. Asiri, F. S. AlMubaddel, and M. M. Rahman, "The fabrication of a chemical sensor with PANI-TiO 2 nanocomposites," *RSC Advances*, vol. 10, no. 21, pp. 12224–12233, 2020.

[15] V. Masoumi, A. Mohammadi, M. Amini, M. R. Khoshayand, and R. Dinarvand, "Electrochemical synthesis and characterization of solid-phase microextraction fibers using conductive polymers: application in extraction of benzaldehyde from aqueous solution," *Journal of Solid State Electrochemistry*, vol. 18, no. 6, pp. 1763–1771, 2014.

[16] G. Inzelt, *Conducting Polymers: A new era in Electrochemistry*, Springer Science & Business Media, 2012.

[17] M. M. Gvozdenović, B. Z. Jugović, D. I. Bezbradica, M. G. Antov, Z. D. Knežević-Jugović, and B. N. Grgur, "Electrochemical determination of glucose using polyaniline electrode modified by glucose oxidase," *Food Chemistry*, vol. 124, no. 1, pp. 396–400, 2011.

[18] S. Ebrahim, R. El-Raey, A. Hefnawy, H. Ibrahim, M. Soliman, and T. M. Abdel-Fattah, "Electrochemical sensor based on polyaniline nanofibers/single wall carbon nanotubes composite for detection of malathion," *Synthetic Metals*, vol. 190, pp. 13–19, 2014.

[19] S. Berhanu, F. Habtamu, Y. Tadesse, F. Gonfa, and T. Tadesse, "Fluorescence sensor based on polyaniline supported Ag-ZnO nanocomposite for malathion detection," *Journal of Sensors*, vol. 2022, Article ID 9881935, pp. 1☐11, 2022.

[20] S. B. Matt, S. Raghavendra, M. Shivanna, M. Sidlinganahalli, and D. M. Siddalingappa, "Electrochemical detection of paracetamol by voltammetry techniques using pure zirconium oxide nanoparticle based modified carbon paste electrode," *Journal of Inorganic and Organometallic Polymers and Materials*, vol. 31, no. 2, pp. 511–519, 2021.

[21] M. Sakthivel, M. Sivakumar, S. M. Chen et al., "A facile synthesis of Cd (OH) 2-rGO nanocomposites for the practical electrochemical detection of acetaminophen," *Electroanalysis*, vol. 29, no. 1, pp. 280–286, 2017.

[22] T. Gete and M. M. Kassaw, "Determination of paracetamol and kinetics Parameters using Nickel hexacynoferrate modified carbon paste electrode," *International Journal of Advanced Research*, vol. 4, no. 12, pp. 1087–1093, 2016.

[23] Z. A. Alothman, N. Bukhari, S. M. Wabaidur, and S. Haider, "Simultaneous electrochemical determination of dopamine and acetaminophen using multiwall carbon nanotubes modified glassy carbon electrode," *Sensors and Actuators B: Chemical*, vol. 146, no. 1, pp. 314–320, 2010.

[24] K. G. B. Alves, J. F. Felix, E. F. de Melo, C. G. dos Santos, C. A. S. Andrade, and C. P. de Melo, "Characterization of ZnO/polyaniline nanocomposites prepared by using surfactant solutions as polymerization media," *Journal of Applied Polymer Science*, vol. 125, no. S1, pp. E141–E147, 2012.

[25] M. Alam, N. M. Alandis, A. A. Ansari, and M. R. Shaik, "Optical and electrical studies of polyaniline/ZnO nanocomposite," *Journal of Nanomaterials*, vol. 2013, Article ID 157810, pp. 1☐5, 2013.

[26] M. Alam, N. M. Alandis, A. A. Ansari, and M. R. Shaik, "Optical and electrical studies of polyaniline/ZnO nanocomposite," *Journal of Nanomaterials*, vol. 2013, Article ID 157810, pp. 1☐5, 2013.

[27] G. R. Yerawar, "Characterization of chemically synthesized polyaniline-zinc oxide nanocomposites," *Der Pharma Chemica*, vol. 4, no. 3, pp. 1288–1291, 2012.

[28] A. Farag, A. Ashery, and M. A. Rafea, "Optical dispersion and electronic transition characterizations of spin coated polyaniline thin films," *Synthetic Metals*, vol. 160, no. 1-2, pp. 156–161, 2010.

[29] B. Meenarathi, A. Thamizhlarasan, L. Kannammal et al., "Effect of polymer structure on the size and shape of metal and metaloxide nanopowder: a HR-TEM approach," *Nano*, vol. 17, no. 07, 2250055, 2022.

[30] K. G. B. Alves, J. F. Felix, E. F. de Melo, C. G. dos Santos, C. A. S. Andrade, and C. P. de Melo, "Characterization of ZnO/polyaniline nanocomposites prepared by using surfactant solutions as polymerization media," *Journal of Applied Polymer Science*, vol. 125, no. S1, pp. E141–E147, 2012.

[31] M. Alam, N. M. Alandis, A. A. Ansari, and M. R. Shaik, "Optical and electrical studies of polyaniline/ZnO nanocomposite," *Journal of Nanomaterials*, vol. 2013, Article ID 157810, pp. 1☐5, 2013.

[32] G. R. Yerawar, "Characterization of chemically synthesized polyaniline-zinc oxide nanocomposites," *Der Pharma Chemica*, vol. 4, no. 3, pp. 1288–1291, 2012.

[33] R. K. Sonker, B. C. Yadav, A. Sharma, M. Tomar, and V. Gupta, "Experimental investigations on NO 2 sensing of pure ZnO and PANI–ZnO composite thin films," *RSC Advances*, vol. 6, no. 61, pp. 56149–56158, 2016.

[34] M. J. Silva, J. Gomes, P. Ferreira, and R. C. Martins, "An overview of polymer-supported catalysts for wastewater treatment through light-driven processes," *Water*, vol. 14, no. 5, p. 825, 2022.

[35] R. Saravanan, E. Sacari, F. Gracia, M. M. Khan, E. Mosquera, and V. K. Gupta, "Conducting PANI stimulated ZnO system for visible light photocatalytic degradation of coloured dyes," *Journal of Molecular Liquids*, vol. 221, pp. 1029–1033, 2016.

[36] A. Olad and R. Nosrati, "Preparation, characterization, and photocatalytic activity of polyaniline/ZnO nanocomposite,"

Research on Chemical Intermediates, vol. 38, no. 2, pp. 323–336, 2012.

[37] V. Gilja, I. Vrban, V. Mandić, M. Žic, and Z. Hrnjak-Murgić, "Preparation of a PANI/ZnO composite for efficient photocatalytic degradation of acid blue," *Polymers*, vol. 10, no. 9, p. 940, 2018.

[38] F. Habtamu, S. Berhanu, and T. Mender, "Polyaniline supported Ag-doped ZnO nanocomposite: synthesis, characterization, and kinetics study for photocatalytic degradation of malachite green," *Journal of Chemistry*, vol. 2021, Article ID 2451836, pp. 1□12, 2021.

[39] A. Jilani, M. O. Ansari, G. u. Rehman et al., "Phenol removal and hydrogen production from water: silver nanoparticles decorated on polyaniline wrapped zinc oxide nanorods," *Journal of Industrial and Engineering Chemistry*, vol. 109, pp. 347–358, 2022.

[40] Z. Zhao, Y. Yang, L. Xu et al., "Amino acid-doped polyaniline nanotubes as efficient adsorbent for wastewater treatment," *Journal of Chemistry*, vol. 2022, Article ID 2041512, pp. 1□12, 2022.

[41] A. A. M. Farag, A. Ashery, and M. A. Rafea, "Optical dispersion and electronic transition characterizations of spin coated polyaniline thin films," *Synthetic Metals*, vol. 160, no. 1-2, pp. 156–161, 2010.

[42] K. M Ziadan, "The electronic transitions of polyaniline doped with p-toluene sulfonic acid," *Journal of Kerbala university*, vol. 1, pp. 67–47, 2005.

[43] S. Kant, S. Kalia, and A. Kumar, "A novel nanocomposite of polyaniline and Fe0. 01Ni0. 01Zn0. 98O: photocatalytic, electrical and antibacterial properties," *Journal of Alloys and Compounds*, vol. 578, pp. 249–256, 2013.

[44] M. Eskezia Ayalew and D. Yenealem Ayitegeb, "Differential pulse voltammetric determination of paracetamol using activated glassy carbon electrode," *American Journal of Physical Chemistry*, vol. 10, no. 2, p. 16, 2021.